# Oscillating Reaction-Diffusion Spots

Aric Hagberg
Center for Nonlinear Studies and T-7, Theoretical Division,
Los Alamos National Laboratory, Los Alamos, NM 87545
(aric@lanl.gov)


Ehud Meron
The Jacob Blaustein Institute for Desert Research and the Physics Department,
Ben-Gurion University, Sede Boker Campus 84990, Israel
(ehud@bgumail.bgu.ac.il)

November 1996

**Abstract**

Reaction-diffusion systems produce a variety of patterns such as spots, labyrinths, and rotating spirals. Circular spots may be stationary or unstable to oscillating motion. The oscillations are sometimes steady but may lead to collapsing or infinitely expanding spots. Using a singular perturbation technique we derive a set of ordinary differential equations for the dynamics of circular spots. These equations are considerably simpler to study than the underlying reaction-diffusion model and quantitatively reproduce the same dynamics.

# 1   Introduction

The discovery of replicating spots, first in models [1] and then in chemical experiments [2, 3] sparked renewed interest in the formation of localized reaction-diffusion patterns. In addition to replicating spots, oscillating circular spots have also been found in the Ferrocyanide-Iodate-Sulfite reaction [4]. One kind of spot is formed from interactions with the circular boundary of the chemical reactor. It may be stationary or become unstable to oscillating (or breathing) motion. Away from the boundary another type of oscillating circular spot may exist [5]. This spot is not significantly influenced by the reactor boundary and exists as a single localized structure.

Theoretical studies of reaction-diffusion models have addressed static and oscillatory instabilities of spots [6, 7], spot splitting [8, 9, 10], and the drifting motion of spots with global coupling [11]. In this article we derive a set of ordinary differential equations to describe the dynamics of circular spots in a two-dimensional reaction-diffusion system. This pair of equations, for an order parameter related to the front speed, and for the curvature of a circular front, describe stationary and oscillating spots and predict the collapse or infinite expansion of unstable spots. This analysis is restricted to the dynamics of circular spots and does not predict instabilites to transverse perturbations that may deform the perfect circular shape.

# 2   Reaction-Diffusion model

The model we consider is an activator-inhibitor reaction-diffusion system describing a bistable medium. Models of this type have been studied in various physical and chemical contexts [12, 13, 14, 15, 16, 17]. The equations, for real scalar fields $u$ and $v$, are

$$
\begin{aligned}
u_t &= \epsilon^{-1}(u - u^3 - v) + \delta^{-1}\nabla^2 u\,, \\
v_t &= u - a_1 v - a_0 + \nabla^2 v\,.
\end{aligned}
\tag{1}
$$

The subscript $t$ denotes the partial time derivative and $\nabla$ is the two-dimensional Laplacian. For $a_1 > 1$ and $a_0 = 0$ the system (1) has two stationary uniform states, $(u_\pm, v_\pm) = \left(\pm\sqrt{1 - 1/a_1}, \pm a_1^{-1}\sqrt{1 - 1/a_1}\right)$. For small $a_0$ the system is still bistable but the parity symmetry $(u, v) \rightarrow (-u, -v)$ is broken.

In addition to the spatially uniform solutions there are also front solutions connecting them. These fronts may be planar (one-dimensional), circular (spots), or irregular (for example in a labyrinth pattern). For planar fronts we consider front solutions that connect $(u_+, v_+)$ at $x = -\infty$ to $(u_-, v_-)$ at $x = \infty$ and are uniform in the $y$ direction. The number and type of these front solutions is determined by the two parameters $\epsilon$ and $\delta$. For $\eta > \eta_c = 3/2\sqrt{2}q^3$, where $\eta = \sqrt{\epsilon\delta}$ and $q^2 = a_1 + 1/2$, a single stable stationary (Ising) front solution exists. This solution loses stability in a pitchfork bifurcation, at $\eta = \eta_c$, to a pair of counterpropagating (Bloch) front solutions [16, 17, 18, 19] as shown in Fig. 1.

In the vicinity of the pitchfork front bifurcation (also called the Nonequilibrium Ising-Bloch, or NIB, bifurcation) small perturbations may influence the front solutions in dramatic ways. In particular, perturbations, such as the curvature of a front, may cause a transition between the counterpropagating solution branches (for $\eta < \eta_c$ in Fig. 1) [10, 20]. Periodic front transitions result in oscillating, or breathing, motion of the fronts. In the next section we show how to derive order parameter equations that describe these transitions.

# 3   Equations for the dynamics of circular fronts

To derive equations for the motion of circular fronts (spots), the first step is to transform into polar coordinates, $r = \rho - \rho_f(t)$, that move with the front. In this frame, and assuming the radius of curvature $\rho_f$ is much larger than the front width, equations (1) are

$$
\begin{aligned}
u_t - (\dot{\rho}_f + (\delta\rho_f)^{-1})u_r &= \epsilon^{-1}(u - u^3 - v) + \delta^{-1}u_{rr}\,, \\
v_t - (\dot{\rho}_f + \rho_f^{-1})v_r &= u - a_1 v - a_0 + v_{rr}\,,
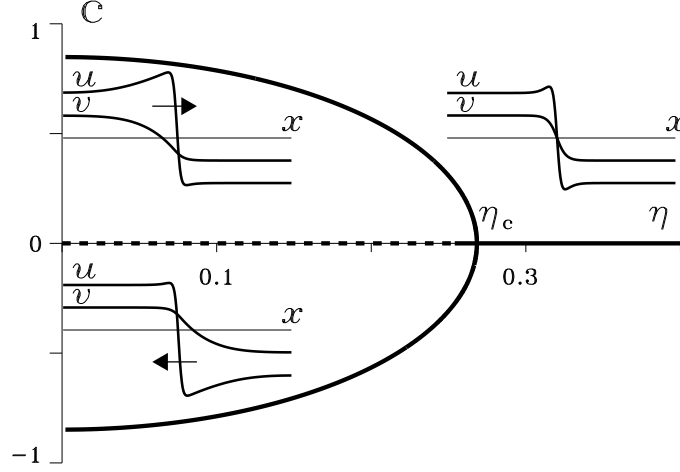\end{aligned}
\tag{2}
$$

Figure 1: The NIB (or nonequilibrium Ising-Bloch) bifurcation when $a_0 = 0$. The pitchfork diagram represents the speed of front solutions $vs$ the parameter $\eta$. For $\eta > \eta_c$, the Ising front is the single solution and $v_f$, the order parameter representing the value of the $v$ field at the front position $u = 0$, is zero. Beyond the bifurcation, $\eta < \eta_c$, a pair of counterpropagating Bloch fronts appears.

where the dot over $\rho_f$ denotes the derivative with respect to $t$. In the following we confine ourselves to the parameter region $\epsilon \ll 1$, $\delta \propto \epsilon^{-1}$ and we choose $\delta$ values such that $\epsilon\delta \sim \mathcal{O}(\eta_c^2)$. The front solution, $u(r,t)$, $v(r,t)$, is characterized by a strong variation of the $u$ field over a distance of order $\sqrt{\mu} = \sqrt{\epsilon/\delta}$, and singular perturbation methods can be used.

Stretching the spatial coordinate, $z = r/\sqrt{\mu}$, to expand this region, equations (2) become

$$\begin{aligned}
\epsilon\left(u_t - \dot{z}_f u_z + (\delta z_f)^{-1} u_z\right) &= u - u^3 - v + u_{zz}\,, \\
\mu\left(v_t - \dot{z}_f v_z + z_f^{-1} v_z - u + a_1 v\right) &= v_{zz}\,,
\end{aligned} \tag{3}$$

where $z_f = \rho_f/\sqrt{\mu}$ and we recall that $\mu \propto \epsilon^2$. Expanding in $\epsilon$

$$\begin{aligned}
u &= u_0 + \epsilon u_1 + \epsilon^2 u_2 + ...\,, \\
v &= v_0 + \epsilon v_1 + \epsilon^2 v_2 + ...\,,
\end{aligned}$$

and inserting into (3) we find at order unity the front solution

$$u_0 = -\tanh(z/\sqrt{2})\,, \qquad v_0 = 0\,.$$

Collecting terms of order $\epsilon$ gives

$$\mathcal{L}u_1 = v_1 - \dot{z}_f u_{0z} - (\delta z_f)^{-1} u_{0z}\,, \qquad \mathcal{L} = \partial_z^2 + 1 - 3u_0^2\,, \tag{4}$$

where $v_1$ is a yet undetermined function of time. Since

$$\mathcal{L}u_{0z} = 0\,,$$

solvability of (4) requires

$$\dot{z}_f + (\delta z_f)^{-1} = -\frac{3}{\sqrt{2}}v_1(t)\,.$$

3

The narrow front region becomes infinitely thin in the limit $\epsilon \to 0$. Therefore, $v(t)$ may be associated with the value of $v(r, t)$ at the front position, that is $v(0, t)$. With this notation the leading order relation is

$$\dot{\rho}_f + \frac{1}{\delta \rho_f} = -\frac{3}{\eta\sqrt{2}} v(0, t) \,. \tag{5}$$

Away from $\rho_f$, $u - u^3 - v \sim \mathcal{O}(\epsilon)$, and $u$ varies on the same time and length scales as $v$. Going back to equations (2) we find at order unity

$$\begin{aligned}
v_t - \dot{\rho}_f v_r + \rho^{-1} v_r &= u_+(v) - a_1 v - a_0 + v_{rr} \,, & r \leq 0 \,, \\
v_t - \dot{\rho}_f v_r + \rho^{-1} v_r &= u_-(v) - a_1 v - a_0 + v_{rr} \,, & r \geq 0 \,,
\end{aligned} \tag{6}$$

where $u_\pm(v)$ are the outer solution branches of the cubic equation $u - u^3 - v = 0$. For $a_1$ sufficiently large we may linearize the branches $u_\pm(v)$ around $v = 0$

$$u_\pm(v) \approx \pm 1 - v/2 \,. \tag{7}$$

Substituting the linearization (7) and the relation from the inner problem (5) into (6) produces the free boundary problem

$$\left. \begin{aligned}
v_t + q^2 v - v_{rr} &= 1 - \frac{3}{\eta\sqrt{2}} v(0, t) v_r + (1 - \delta^{-1}) v_r / \rho_f - a_0 \\
v(-\infty, t) &= v_+ \approx q^{-2}
\end{aligned} \right\} \quad r \leq 0 \,, \tag{8}$$

$$\left. \begin{aligned}
v_t + q^2 v - v_{rr} &= -1 - \frac{3}{\eta\sqrt{2}} v(0, t) v_r + (1 - \delta^{-1}) v_r / \rho_f - a_0 \\
v(\infty, t) &= v_- \approx -q^{-2}
\end{aligned} \right\} \quad r \geq 0 \,,$$

$$[v]_{r=0} = [v_r]_{r=0} = 0 \,, \tag{9}$$

where the square brackets in (9) denote jumps across the free boundary.

Equations (8) can be solved by assuming that the system is near the front bifurcation and expanding in powers of the front speed $c$. If we require that the last two terms ($a_0$ and the term with $\rho_f$) in Eqns. (8) are of order $c^3$ this expansion gives a series of equations that produce as a compatibility condition the order parameter equation

$$\dot{v}_f = \frac{\sqrt{2}}{q\eta_c^2} (\eta_c - \eta) v_f - \frac{3}{4\eta_c^2} v_f^3 - \frac{2}{3q} \frac{(1 - \delta^{-1})}{\rho_f} - \frac{4}{3} a_0 \,. \tag{10}$$

where $v_f(t) = v(0, t)$, is the value of the inhibitor at the front position $\rho_f(t)$. The order parameter $v_f$ is related to the speed of a front (see Fig. 1).

The full details of the solution technique can be found in Ref. [21].

# 4 Collapsing, expanding, and oscillating spots

Writing equations (5) and (10) terms of the curvature $\kappa = \rho_f^{-1}$ gives the equations

$$\begin{aligned}
\dot{v}_f &= \frac{\sqrt{2}}{q\eta_c^2} (\eta_c - \eta) v_f - \frac{3}{4\eta_c^2} v_f^3 - \frac{2}{3q} (1 - \delta^{-1}) \kappa - \frac{4}{3} a_0 \,, \\
\dot{\kappa} &= \frac{3}{\eta\sqrt{2}} v_f \kappa^2 + \delta^{-1} \kappa^3 \,,
\end{aligned} \tag{11}$$

that describe the dynamics of large circular spots. Consider first the fixed point solutions obtained by the intersections of the linear nullclines $\kappa = 0$ and $\kappa = -(3\delta/\eta\sqrt{2}) v_f$ of the bottom equation in (11) with the cubic nullcline of the top equation in (11). The solutions corresponding to $\kappa = 0$ describe planar fronts propagating at constant velocities. Solutions with positive and negative $v_f$ values pertain to down states invading up states and up states invading down

4

states, respectively. The number of $\kappa = 0$ solutions varies with $\eta$. Below the front bifurcation, $[\eta > \eta_c(a_0)]$, there is a single intersection point representing an Ising front as shown by the thin lines in Fig. 2a and Fig. 2b. Beyond the front bifurcation, $[\eta < \eta_c(a_0)]$, two more intersection points appear corresponding a stable and unstable pair of planar front solutions (Fig. 2c). The fixed point solutions for $\kappa \neq 0$ represent a circular fronts. For $a_0 < 0$ they describe spots of up an state domain and for $a_0 > 0$ spots of a down state domain. For $\delta > 1$, depending on the choice of $\epsilon$, these fixed points may or may not be stable. For $\delta < 1$, all the $\kappa \neq 0$ fixed points are *unstable*.

Fig. 2 shows three different possibilities for the dynamics of circular fronts. The thick trajectories represent dynamics computed by numerical solution of the coupled equations (11). The initial conditions correspond to a large shrinking up state spot. Far into the Ising regime (Fig. 2a). the initial spot converges to a stationary spot. Moving closer to the front bifurcation and past a critical $\eta$ value, $\eta_H > \eta_c(a_0)$, a Hopf bifurcation to a breathing spot occurs (Fig. 2b). Crossing the front bifurcation, $\eta < \eta_c(a_0)$, the spot rebounds, i.e. the shrinking spot reaches a minimal size and expands again indefinitely (Fig. 2c). For larger $|a_0|$, there is another possibility for the dynamics of spots. In this case, shown in Fig. 3, the amplitude of oscillations grows in time until the spot eventually collapses as the curvature diverges to infinity. Note that the equations (11) are not valid for studying the final collapse of the spot since the curvature is high and the equations are not valid then. They do, however, predict the onset of collapse.

All three dynamical behaviors discussed above have been observed in direct simulations of (1). The quantitative accuracy of the order parameter equations was tested by computing numerical solutions to the circularly symmetric version of equations (1)

$$
\begin{aligned}
u_t &= \epsilon^{-1}(u - u^3 - v) + \frac{\delta^{-1}}{r}u_r + \delta^{-1}u_{rr}\,, \\
v_t &= u - a_1 v - a_0 + \frac{1}{r}v_r + v_{rr}\,.
\end{aligned}
\tag{12}
$$

and comparing them to solutions to equations (11) for spot dynamics. Spot solutions of (12) produce the same qualitative behavior as the pair of coupled equations for the spot dynamics. When the parameters are chosen to satisfy the assumptions made in the derivation of (11), there is also quantitative agreement between the two solutions. Fig. 4 shows the curvature of an oscillating spot as a function of time computed using both equations (11) and (12). The two solutions agree within an accuracy of approximately 1% for the amplitude and 2% for the phase.

## 5 Conclusion

We have shown how the dynamics of circular spots in a reaction-diffusion system can be studied through the use of a pair of ordinary differential equations. These equations predict collapsing, expanding and oscillating spots. In addition to the oscillatory instability spot solutions may also be unstable to transverse perturbations [6, 22, 23]. Numerical solutions of the fully two-dimensional model (1) show that for the parameters of Fig. 4 spots are unstable and form nonuniformly curved fronts leading to a labyrinthine pattern. Since the order parameter equations derived here apply only for the case when the spots do not break perfect circular symmetry, for this choice of parameters they only capture the dynamics of the circular spot during the initial evolution. Order parameter equations for the dynamics of nonuniformly curved fronts are discussed in Ref. [24].

## References

[1] J. E. Pearson, Science **261**, 189 (1993).

[2] K. J. Lee, W. D. McCormick, Q. Ouyang, and H. L. Swinney, Science **261**, 192 (1993).

[3] K. J. Lee, W. D. McCormick, J. E. Pearson, and H. L. Swinney, Nature **369**, 215 (1994).

[4] D. Haim, G. Li, Q. Ouyang, W. D. McCormick, H. L. Swinney, A. Hagberg, and E. Meron, Phys. Rev. Lett. **77**, 190 (1996).

[5] G. Li, Q. Ouyang, and H. L. Swinney, "Transitions in 2D patterns in a Ferrocyanide-Iodate-Sulfite reaction", submitted to *J. Chem. Phys. (1996)* (unpublished).

[6] T. Ohta, M. Mimura, and R. Kobayashi, Physica D **34**, 115 (1989).

[7] C. B. Muratov and V. V. Osipov, Phys. Rev. E **53**, 3101 (1996).

[8] W. N. Reynolds, J. E. Pearson, and S. Ponce-Dawson, Phys. Rev. Lett. **72**, 2797 (1994).

[9] A. Hagberg and E. Meron, Chaos **4**, 477 (1994).

[10] C. Elphick, A. Hagberg, and E. Meron, Phys. Rev. E **51**, 3052 (1995).

[11] K. Krischer and A. Mikhailov, Phys. Rev. Lett. **73**, 3165 (1994).

[12] J. J. Tyson and J. P. Keener, Physica D **32**, 327 (1988).

[13] E. Meron, Physics Reports **218**, 1 (1992).

[14] M. Bär, S. Nettesheim, H. H. Rotermund, M. Eiswirth, and G.Ertl, Phys Rev. Lett. **74**, 1246 (1995).

[15] G. Haas, M. Bär, I. G. Kevrekidis, P. B. Rasmussen, H.-H. Rotermund, and G.Ertl, Phys Rev. Lett. **75**, 3560 (1995).

[16] M. Bode, A. Reuter, R. Schmeling, and H.-G. Purwins, Phys Lett. A **185**, 70 (1994).

[17] P. Schütz, M. Bode, and H.-G. Purwins, Physica **82D**, 382 (1995).

[18] A. Hagberg and E. Meron, Nonlinearity **7**, 805 (1994).

[19] H. Ikeda, M. Mimura, and Y. Nishiura, Nonl. Anal. TMA **13**, 507 (1989).

[20] A. Hagberg, E. Meron, I. Rubinstein, and B. Zaltzman, Phys. Rev. Lett. **76**, 427 (1996).

[21] A. Hagberg, E. Meron, I. Rubinstein, and B. Zaltzman, submitted to *Phys. Rev. E* (unpublished).

[22] D. M. Petrich and R. E. Goldstein, Phys. Rev. Lett. **72**, 1120 (1994).

[23] R. E. Goldstein, D. J. Muraki, and D. M. Petrich, Phys. Rev. E **53**, 3933 (1996).

[24] A. Hagberg and E. Meron, "The dynamics of curved fronts: beyond geometry", preprint (1996) (unpublished).
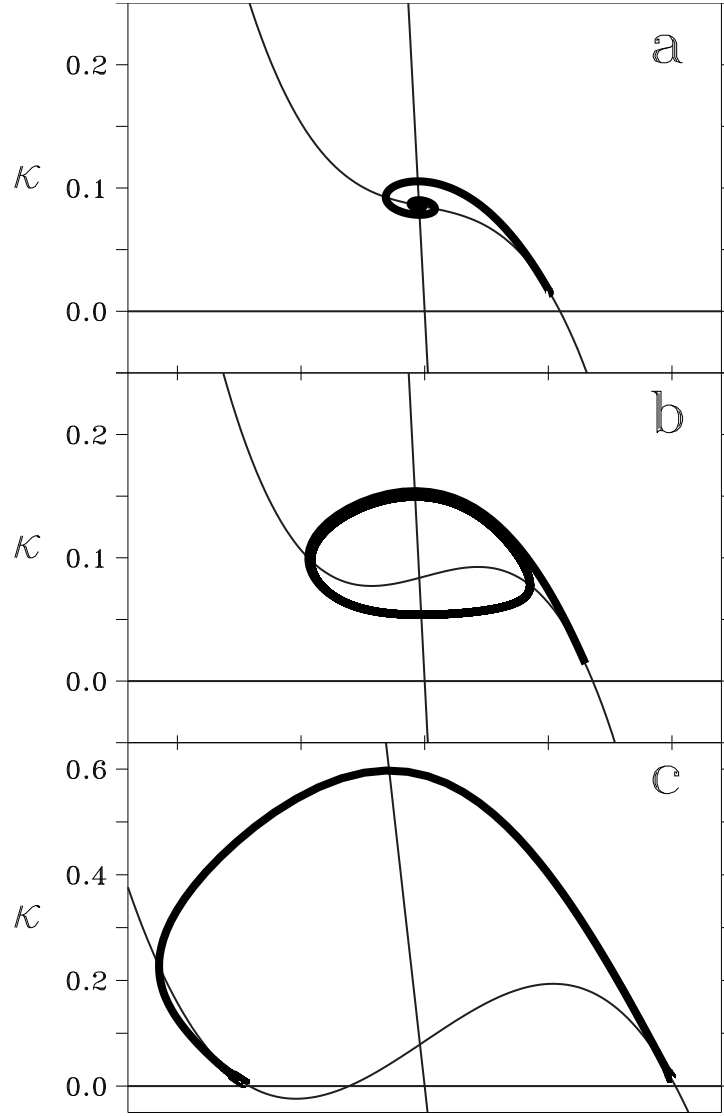
Figure 2: Three types of solutions to the order parameter equations (11) starting with initial conditions representing a large shrinking spot. The thin lines are the isoclines and the thick lines are numerically computed trajectories. (a) Convergence to a stationary spot ($\epsilon = .0063$). (b) An oscillating spot ($\epsilon = .006$). (c) Spot rebound and expansion of the spot to infinite size ($\epsilon = .0052$). Parameters: $a_1 = 4.0$, $a_0 = -0.01$, and $\delta = 2.0$.
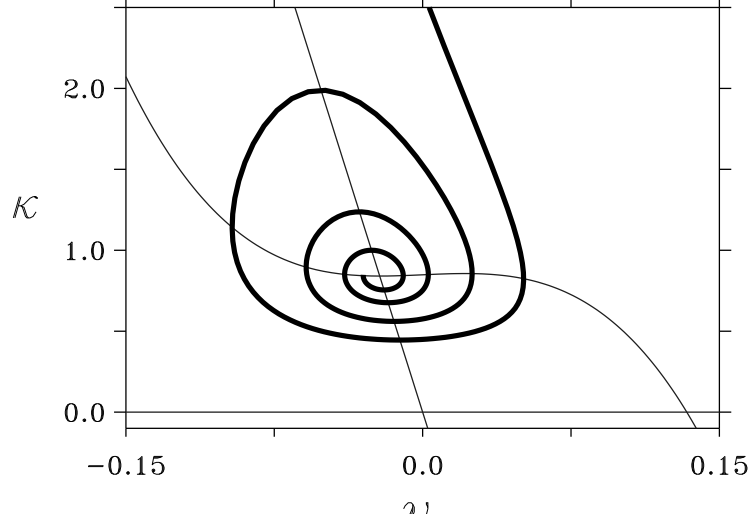
Figure 3: A trajectory of the order parameter equations (11) for a spot that oscillates with growing amplitude until collapse (the curvature $\kappa$ diverges to infinity). Parameters: $a_1 = 4.0$, $a_0 = -0.1$, $\epsilon = 0.006$, and $\delta = 2.0$.
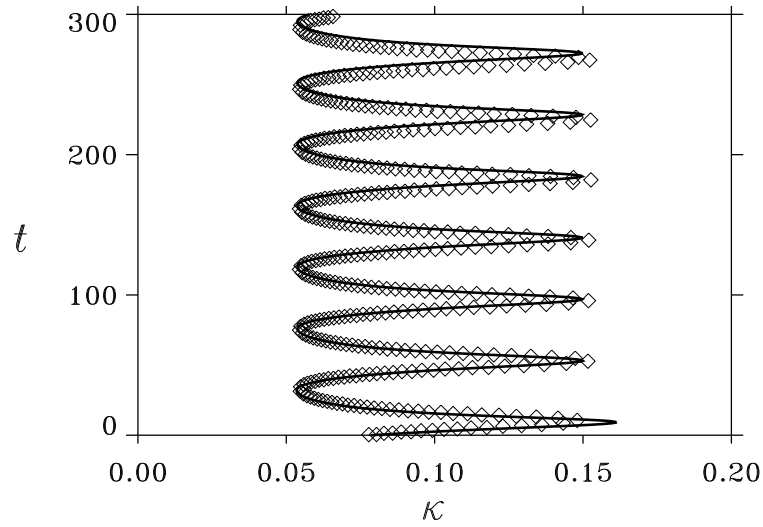


Figure 4: An oscillating circular spot solution. The solid line is the solution of the order parameter equations (11), and the diamonds represent the spot curvature vs time from the numerical solution to the circularly symmetric equations (12). The equation parameters are $\epsilon = 0.006$, $\delta = 2.0$, $a_1 = 4.0$, $a_0 = -0.01$.